Geochemical Journal, Vol. 32, pp. 71 to 89, 1998

Estimation of oxygen diffusivity from anion porosity in minerals

YONG-FEI ZHENG and BIN FU

Department of Earth and Space Sciences, University of Science and Technology of China, Hefei 230026, P.R. China

(Received June 18, 1996; Accepted September 26, 1997)

An empirical model for predicting oxygen diffusivity from anion porosity is presented for a wide range of minerals. It is based on the examination of experimental diffusion data under anhydrous and hydrothermal conditions. The relationship between activation energies and pre-exponential factors in all minerals is assumed to obey a common compensation law regardless of diffusion medium (H_2O, OH^-, CO_2 or O_2). However, the H_2O molecules and OH^- groups are relatively small in volume and thus can migrate within mineral structures with given anion porosities easier than the CO_2 and O_2. As a result, the rates of oxygen diffusion in minerals under hydrothermal conditions are greater than those under anhydrous conditions. The Arrhenius parameters for oxygen diffusion in about 130 minerals have been estimated for the anhydrous and hydrothermal conditions, respectively. The empirical results on oxygen diffusivity are internally consistent for the minerals of geochemical interest and thus can be applicable to oxygen isotope geospeedometry during cooling of high-temperature mineral assemblages.

INTRODUCTION

The role of diffusion in geological processes has been the subject of growing interest in the last two decades. The importance of intercrystalline diffusion in metamorphic reactions was recognized for a long time. Knowledge of chemical diffusion rates systematized in terms of the crystal structure and chemical composition of minerals is fundamental to quantitative study of various pressure-temperature-time (P-T-t) evalution in geological processes. Successful application of geothermometers and geobarometers has to take into account different inter- and intra-crystalline equilibrium controlled by diffusion processes. Of general significance is the extent to which mineral grains are able to maintain mutual chemical equilibrium by diffusion, and when the isotopic compositions of minerals become fixed, or frozen in, during the cooling of high-temperature rock. In order to achieve such objectives, it is essential to characterize diffusion parameters in minerals. Experimentally determined diffusion data for important elements in rock-forming minerals have being grown recently (e.g., Freer, 1981; Giletti and Yund, 1984; Cole and Ohmoto, 1986; Farver and Giletti, 1989; Sharp *et al.*, 1991; Farver, 1994; Ryerson and McKeegan, 1994). Nevertheless, they are still considerably less abundant than what is required in geochemical applications because of difficulties in laboratory investigations.

Sharp (1991) developed a technique for correlating crystal grain size with the oxygen isotope compositions of a silicate or oxide mineral hosted by a marble in order to quantify the diffusion coefficients of oxygen in that mineral. Recent efforts using atomistic simulation methods have proven very promising in predicting the structural, thermodynamic, point defect and diffusional properties of a range of minerals (e.g., Catlow and Price, 1990; Purton and Catlow, 1990; Patel *et al.*, 1991; Wright and Catlow, 1994; Vocadlo *et al.*, 1995; Wright *et al.*, 1996). By defining an interatomic potential function to describe the total energy of a system in terms of atomic positions, the atomistic approach has been employed by Wright *et al.* (1995) to investigate the diffusion of oxygen and hydroxyl groups in grossular garnet. However, the

methodology used does not allow the calculation of absolute diffusion rates. In this regard, there is no established model to theoretically predict the diffusion coefficients of ionic species in minerals.

Oxygen is the most abundant element in the Earth. Study of the rates of oxygen exchange by self-diffusion in rock-forming minerals can provide important data for the interpretation of thermal histories in geological processes (e.g., Giletti, 1985, 1986). Meanwhile, oxygen is the largest ion in most minerals and thus its mobility itself controls the nature of oxygen transport and exchange within mineral crystal structure. Obviously, the mineral structure is the dominant control of oxygen diffusivity. Dowty (1980) suggested that anion porosity, electrostatic site energy and ionic size can affect the mobility of ions in minerals. Connolly and Muehlenbachs (1988) observed that anion porosity is proportional to the activation energy of oxygen diffusion. Muehlenbachs and Connolly (1991) examined published data for anhydrous oxygen diffusion and proposed a simple relationship to predict oxygen diffusion coefficients based on anion porosity. Fortier and Giletti (1989) presented a similar relationship for estimating hydrothermal oxygen diffusivity from total ionic porosity. Therefore, rates of oxygen diffusion in minerals are principally controlled by the void space in the crystal.

In the absence of a quantitative theory, it is highly desirable to have empirical models that can be used to predict diffusion coefficients (D) where experimental data are lacking. Voltaggio (1985) presented a method based on the isokinetic effects, an analogy to the compensation law of Winchell (1969) which relies on observed correlations between $\ln D_0$, the natural logarithm of the pre-exponential factor in Arrhenius diffusion relation $D = D_0\exp(-Q/RT)$, and Q, the activation energy. Alternatively, oxygen diffusivity in crystalline minerals has been demonstrated by Fortier and Giletti (1989) and Muehlenbachs and Connolly (1991) to be intrinsically correlated with ionic porosity. The accurate calculation of ionic porosity and the recent acquisition of additional diffusion data from laboratory measurements makes it possible to develop their approaches further. This study presents a generalized model for the empirical prediction of oxygen diffusion coefficients in minerals under anhydrous and hydrothermal conditions, respectively.

Methodology

Dowty (1980) suggested that anion porosity gives a direct measure of atomic packing density in the crystal structure of minerals and thus it has a strong influence on ionic diffusion through a given structure. The anion porosity is thus defined as the percentage of unit cell volume not occupied by anion according to the expression:

$$\Phi = (1 - V_A/V_C) \times 100, \quad (1)$$

where V_C is the volume of the unit cell, and V_A is the volume of anions in the unit cell which is calculated by use of anion radii and assumption of spherical geometry. Calculated from compositional and unit-cell data, Φ is a first-order monitor of both M-O bond length/strength and diffusivity of anion among different mineral structures. The smaller the Φ values, the closer the atomic spacings and thus the stronger the cation-oxygen bonds in minerals.

Since the volume of the unit cell is accurately known for crystalline minerals, the accuracy of calculated anion porosities is determined by the values of anion radii. In the previous calculations of Dowty (1980), the ionic radius of oxygen was assumed to be 1.36 Å throughout. Fortier and Giletti (1989) set the ionic radius of oxygen equal to 1.38 Å. However, Shannon and Prewitt (1969) have shown that both cation and anion radii vary with coordination number. Because oxygen has different coordination numbers with respect to cations in the crystal structure of minerals, it is a simplification to assume the same ionic radius of oxygen in calculating the volume of either anions or total ions in the unit cell.

With respect to the absolute values of ionic radii, there are the two sets of radii available in literature: (1) the traditional radii based on

$r(^{VI}O^{2-})$ = 1.40 Å; (2) the crystal radii based on $r(^{VI}O^{2-})$ = 1.26 Å and $r(^{VI}F^{-})$ = 1.19 Å (Shannon and Prewitt, 1969; Shannon, 1976). The crystal radii differ from the traditional radii only by a constant factor of 0.14 Å, as listed in Table 1 for O^{2-}, $(OH)^{-}$ and F^{-}. Shannon (1976) pointed out that the crystal radii defined by Fumi and Tosi (1964) correspond more closely to the physical size of ions in a solid. Therefore, they should be used for the closest packed structure in spheres (Muller and Roy, 1974) and diffusion in solids (Flygare and Haggins, 1973). For this reason, the crystal radii are used in the present study. The unit cell volume are taken either directly from Smyth and Bish (1988) or computed by use of the cell parameters given in Berry *et al.* (1983).

Winchell (1969) suggested that diffusion in silicate glasses obeys the compensation law in the Arrhenius relation, i.e. diffusion of different species shows a positive correlation between $\ln D_0$ and Q. A similar effect was noted by Hofmann (1980) for cation diffusion in basalt. Hart (1981) demonstrated that various diffusion species in silicate minerals exhibit a well-defined compensation effect. These imply that diffusion rates of different species tend to converge at a particular temperature regardless of diffusion medium.

Table 1. Effective ionic radii (after Shannon, 1976)

Anion	CN	CR (Å)	IR (Å)
O^{2-}	II	1.21	1.35
	III	1.22	1.36
	IV	1.24	1.38
	VI	1.26	1.40
	VIII	1.28	1.42
OH^{-}	II	1.18	1.32
	III	1.20	1.34
	IV	1.21	1.35
	VI	1.23	1.37
F^{-}	II	1.145	1.285
	III	1.16	1.30
	IV	1.17	1.31
	VI	1.19	1.33

CN: coordination number, CR: crystal radius, IR: traditional radius.

The Arrhenius parameters for oxygen self-diffusion in a number of minerals have been experimentally determined by isotopic exchange under anhydrous "dry" and/or hydrothermal "wet" conditions. The anhydrous diffusion implies the exchange with a nominally anhydrous gas, either O_2 or CO_2 (e.g., Anderson, 1969; Muehlenbachs and Kushiro, 1974; Kronenberg *et al.*, 1984; Sharp *et al.*, 1991), whereas the hydrothermal diffusion means the exchange with water enriched in ^{18}O at high pressures (e.g., Giletti *et al.*, 1978; Freer and Dennis, 1982; Farver and Giletti, 1985; Fortier and Giletti, 1991). More than two sets of experimental data have been reported for some of the minerals (e.g., quartz, forsterite) under the same conditions. Freer and Dennis (1982) recognized that oxygen diffusion under anhydrous conditions was associated with slow diffusivities and high activation energies while oxygen diffusion under hydrothermal conditions was associated with faster diffusion rates and small activation energies.

Figure 1 illustrates a common compensation trend between $\ln D_0$ (in cm^2/sec) and Q (in KJ/mol) for oxygen self-diffusion in minerals under the anhydrous and hydrothermal (P_{H_2O} = 1 kbar) conditions. Table 2 lists the representative data plotted in Fig. 1 on the activation energies and the pre-exponential factors. The experimental data for oxygen diffusion in quartz and forsterite are not included in plotting Fig. 1. This is on the one hand because there is a wide variation in oxygen self-diffusion rates of quartz and forsterite depending upon the experimental technique and exchange medium (Ando *et al.*, 1981; Jaoul *et al.*, 1983; Farver and Yund, 1991; Sharp *et al.*, 1991). On the other hand, the purpose for this is to test whether the present study can independently provide a reasonable estimate of oxygen diffusivity in both minerals. Nevertheless, inclusion of the experimental data for both quartz and forsterite does not considerably improve the compensation trend in Fig. 1.

The common compensation trend in Fig. 1 suggests that oxygen will approach the same diffusion rate in minerals under either anhydrous or hydrothermal conditions at a given temperature.

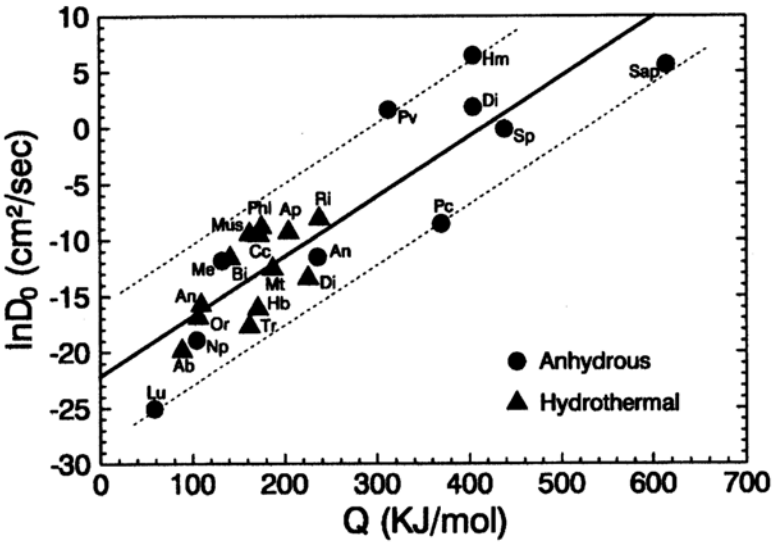

Fig. 1. The compensation plot of activation energies versus pre-exponential factors for oxygen diffusion under anhydrous and hydrothermal conditions. Solid line denotes the best fit to the experimental data, dashed lines are used to bracket the variation range in the intercept of the compensation line. Abbreviations and references are given in Table 2.

Table 2. Arrhenius parameters for oxygen self-diffusion in minerals

Mineral	Φ (%)	Q (KJ/mol)	$\ln D_0$ (cm^2/sec)	Reference
Anhydrous experiments				
Leucite (Lu)	69.78	59	−25.07	Muehlenbachs and Connolly (1991)
Nepheline (Np)	67.23	105	−18.95	Connolly and Muehlenbachs (1988)
Anorthite (An)	64.48	236	−11.51	Elphick *et al.* (1988)
Melilite (Me)	63.66	133	−11.84	Hayashi and Muehlenbachs (1986)
Diopside (Di)	57.01	405	1.84	Connolly and Muehlenbachs (1988)
Periclase (Pc)	55.14	370	−8.57	Reddy and Cooper (1983)
Perovskite (Pv)	55.01	313	1.61	Gautason and Muehlenbachs (1993)
Hematite (Hm)	52.54	405	6.45	Reddy and Cooper (1983)
Spinel (Sp)	51.63	439	−0.12	Ando and Oishi (1974)
Sapphire (Sap)	43.61	615	5.60	Reddy and Cooper (1982)
Hydrothermal experiments				
Orthoclase (Or)	67.01	107	−16.91	Giletti *et al.* (1978)
Anorthite (An)	64.48	110	−15.79	Giletti *et al.* (1978)
Albite (Ab)	64.42	89	−19.89	Giletti *et al.* (1978)
Calcite (Cc)	62.80	173	−9.57	Farver (1994)
Philogopite (Phl)	62.64	176	−8.87	Fortier and Giletti (1991)
Biotite (Bi)	62.20	142	−11.61	Fortier and Giletti (1991)
Muscovite (Mus)	62.01	163	−9.47	Fortier and Giletti (1991)
Apatite (Ap)	60.99	205	−9.32	Farver and Giletti (1989)
Tremolite (Tr)	59.54	163	−17.73	Farver and Giletti (1985)
Hornblende (Hb)	59.15	172	−16.12	Farver and Giletti (1985)
Richterite (Ri)	58.67	238	−8.11	Farver and Giletti (1985)
Diopside (Di)	57.01	226	−13.41	Farver (1989)
Magnetite (Mt)	56.81	188	−12.56	Giletti and Hess (1988)

Furthermore, a similar mechanism of oxygen diffusion may be operative in these diverse minerals regardless of the diffusion medium. The compensation trend in Fig. 1 can be algebraically represented by the following linear equation:

$$\ln D_0 = 0.0534\ (\pm 0.0062)Q - 22.15\ (\pm 3.96), \quad (2)$$

where the figures in brackets denote the statistical errors (1σ). The linear correlation in Fig. 1 may be improved if the experimental data are taken from the same laboratory by means of the same analytical technique on both natural and synthetic samples.

As a result of the compensation effect, all the Arrhenius lines intersect at a single value for the diffusion coefficient at a given critical temperature. The critical temperature (T_c) and diffusion coefficient (D_c) can be calculated from Eq. (2), which are 1980°C and 2.4×10^{-10} cm^2/sec, respectively. This implies that, at about 2000°C, oxygen will diffuse at the same rates of 2.4×10^{-10} cm^2/sec in all the crystalline minerals regardless of their anion porosity and the diffusion medium. The similar conclusion has been reached by Gautason and Muehlenbachs (1993) for the anhydrous oxygen diffusion.

Figure 2 illustrates high degrees of negative correlation between anion porosity (Φ) and activation energy (Q) experimentally determined under the anhydrous and hydrothermal conditions, respectively. It appears that with decreasing anion porosity the activation energies of oxygen self-diffusion under anhydrous conditions are progressively greater than those under hydrothermal conditions. The linear trends in Fig. 2 can be algebraically represented by the following equations:

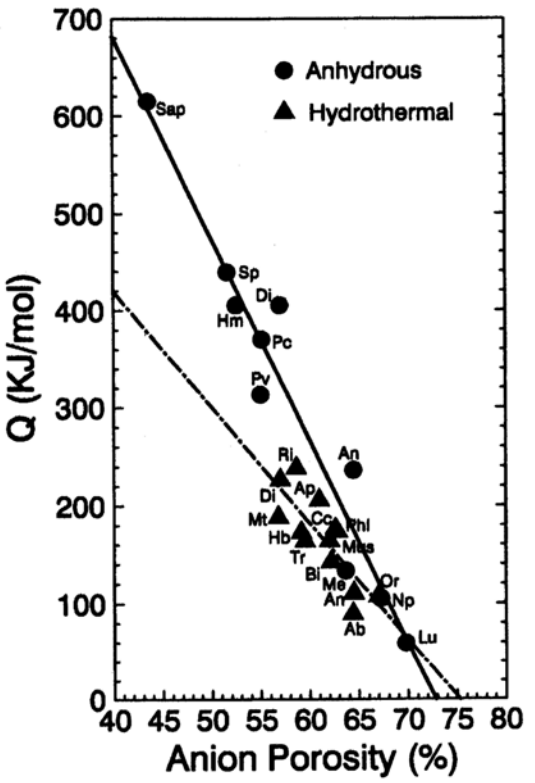

Fig. 2. The observed relation of activation energies for oxygen diffusion under anhydrous and hydrothermal conditions to anion porosities in minerals. Abbreviations and references are given in Table 2.

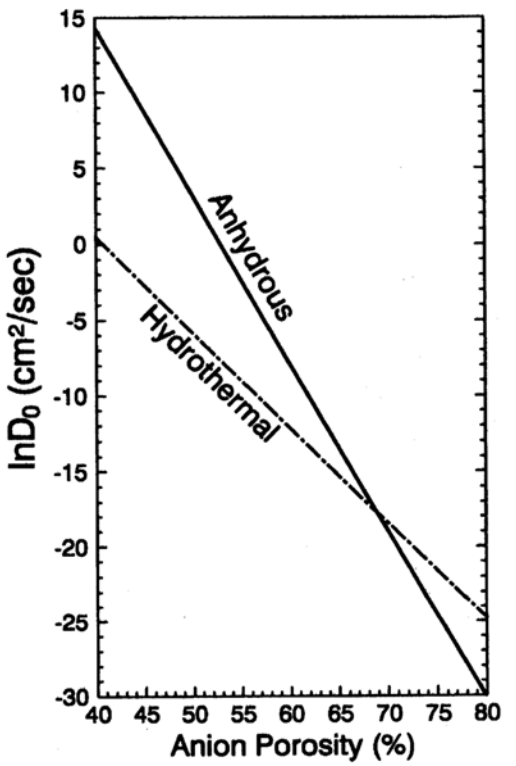

Fig. 3. The relation of anion porosities to pre-exponential factors for oxygen diffusion in minerals under anhydrous and hydrothermal conditions.

$$Q^{dry} = -20.78\ (\pm 1.88)\Phi + 1513.4\ (\pm 22.9), \quad (3)$$

and

$$Q^{wet} = -11.89\ (\pm 2.62)\Phi + 894.9\ (\pm 13.9), \quad (4)$$

where the superscripts *dry* and *wet* denote the anhydrous and hydrothermal conditions, respectively.

In general, the presence of water causes the diffusion rates of oxygen in minerals to be higher and activation energies lower. Because oxygen could migrate in wet conditions as either H_2O molecules or OH^- groups, the higher diffusion rates for oxygen isotope exchange in wet conditions relative to dry conditions are probably related to the independent mobility of the water molecules or hydroxyl groups in mineral structure. The wa-

Table 3. Anion porosity and oxygen diffusivity predicted for metal oxides and hydroxides

Mineral	V_A (Å)	V_C (Å)	Φ (%)	Q^{dry}	$\ln D_0^{dry}$	Q^{wet}	$\ln D_0^{wet}$
Ulvospinel	255.44	621.96	58.91	289	–6.72	194	–11.47
Jacobsite	255.44	616.51	58.57	296	–6.34	199	–11.25
Magnetite	255.44	591.43	56.81	333	–4.39	219	–10.15
Chromite	255.44	588.31	56.58	338	–4.13	222	–10.01
Magnesioferrite	255.44	584.28	56.28	344	–3.80	226	–9.82
Hercynite	255.44	542.50	52.91	414	–0.06	266	–7.69
Spinel	255.44	528.14	51.63	441	1.36	281	–6.89
Mg_2SiO_4 (sp)	255.44	524.56	51.30	447	1.73	285	–6.68
Ni_2SiO_4 (sp)	255.44	520.49	50.92	455	2.15	289	–6.44
Ilmenite	143.68	315.84	54.51	381	–1.84	247	–8.70
Hematite	143.68	302.72	52.54	422	0.35	270	–7.46
$MgSiO_3$ (il)	143.68	265.54	45.27	573	8.42	357	–2.88
Corundum	143.68	254.80	43.61	607	10.26	376	–1.83
Perovskite	100.50	223.33	55.00	371	–2.38	241	–9.01
$MgSiO_3$ (pv)	100.50	162.35	38.10	722	16.38	422	1.64
Thorianite	63.86	175.69	63.63	191	–11.96	138	–14.45
Uraninite	63.86	163.51	60.94	247	–8.97	170	–12.75
Cassiterite	30.41	71.74	57.45	320	–5.10	212	–10.55
Baddeleyite	60.82	140.45	56.70	335	–4.27	220	–10.08
Rutile	30.41	62.07	51.01	453	2.05	288	–6.50
Pyrolusite	30.41	55.48	45.19	574	8.51	358	–2.83
Lime	33.50	111.32	69.91	61	–18.93	64	–18.40
Zincite	15.96	47.31	66.25	137	–14.87	107	–16.10
Manganosite	33.50	87.88	61.88	228	–10.02	159	–13.34
Tenorite	31.93	81.08	60.62	254	–8.62	174	–12.55
Wuestite	33.50	80.11	58.18	304	–5.91	203	–11.01
Periclase	33.50	74.67	55.14	368	–2.54	239	–9.10
Bunsenite	33.50	72.43	53.75	396	–0.99	256	–8.22
Bromellite	15.96	26.97	40.82	665	13.36	410	–0.08
Brucite	14.47	40.75	64.49	173	–12.91	128	–14.99
Gibbsite	165.09	427.98	61.43	237	–9.52	164	–13.06
Goethite	59.35	137.43	56.82	332	–4.40	219	–10.16
Manganite	118.70	270.95	56.19	346	–3.70	227	–9.56
Boehmite	59.35	129.30	54.10	389	–1.38	252	–8.44
Diaspore	59.35	117.96	49.69	481	3.51	304	–5.66

Table 4. Anion porosity and oxygen diffusivity predicted for anhydrous silicates

Mineral	V_A (Å)	V_C (Å)	Φ (%)	Q^{dry}	$\ln D_0^{dry}$	Q^{wet}	$\ln D_0^{wet}$
Tridymite	712.03	2110.2	66.26	137	−14.88	107	−16.10
Cristobalite	59.34	172.17	65.54	151	−14.08	116	−15.65
β-Quartz	44.50	118.12	62.30	219	−10.48	154	−13.61
α-Quartz	44.50	113.01	60.62	254	−8.62	174	−12.55
Coesite	237.34	548.76	56.74	334	−4.31	220	−10.11
Stishovite	30.41	46.54	34.66	793	20.20	483	3.80
Rb-feldspar	237.34	736.01	67.75	106	−16.53	89	−17.04
Celsian	474.68	1466.9	67.64	108	−16.41	91	−16.97
Orthoclase	237.34	719.13	67.01	121	−15.71	98	−16.58
Sanidian	237.34	717.15	66.91	123	−15.60	99	−16.51
Anorthite	474.68	1336.4	64.48	174	−12.90	128	−14.98
Albite	237.34	667.12	64.42	175	−12.84	129	−14.94
Kalsilite	59.34	200.40	70.39	51	−19.46	58	−18.71
Leucite	712.03	2356.0	69.78	63	−18.79	65	−18.32
Nepheline	237.34	724.19	67.23	116	−15.96	96	−16.71
Andalusite	152.05	342.44	55.60	358	−3.05	234	−9.39
Sillimanite	151.30	332.29	54.47	382	−1.79	247	−8.68
Kyanite	153.57	293.72	47.72	522	5.71	328	−4.42
Cordierite	542.92	1554.77	65.08	161	−13.57	121	−15.36
Melilite	111.75	307.55	63.66	191	−11.99	138	−14.47
Beryl	271.46	674.89	59.78	271	−7.69	184	−12.02
Hedenbergite	188.54	450.72	58.17	305	−5.90	203	−11.01
Ferrosilite	370.99	875.85	57.64	316	−5.31	210	−10.67
Diopside	188.54	438.58	57.01	329	−4.61	217	−10.28
Acmite	188.54	429.06	56.06	348	−3.56	228	−9.68
Ca-Tschermaks	185.49	421.35	55.98	350	−3.48	229	−9.63
Enstatite	370.99	832.49	55.44	361	−2.87	236	−9.28
Omphacite	188.54	415.10	54.58	379	−1.91	246	−8.75
Jadeite	188.54	401.85	53.08	410	−0.25	264	−7.80
Spodumene	188.49	389.15	52.33	426	0.58	273	−7.33
Wollastonite	278.24	788.04	64.69	169	−12.91	126	−15.11
Bustamite	278.24	764.30	63.60	192	−11.93	139	−14.43
Rhodonite	228.07	579.84	60.67	253	−8.67	174	−12.58
Andradite	766.31	1753.2	56.29	344	−3.81	226	−9.82
Uvarovite	766.31	1722.8	55.52	360	−2.96	235	−9.34
Grossular	766.31	1661.9	53.89	394	−1.15	254	−8.31
Spessartine	766.31	1565.7	51.06	452	1.99	288	−6.53
Almandine	766.31	1533.2	50.02	474	3.15	300	−5.87
Pyrope	766.31	1504.7	49.07	494	4.20	311	−5.27
Monticellite	127.72	341.84	62.64	212	−10.86	150	−13.82
Tephroite	127.72	325.02	60.70	252	−8.71	173	−12.60
Kirschsteinite	127.72	314.89	59.44	278	−7.31	188	−11.81
Fayalite	127.72	307.42	58.45	299	−6.21	200	−11.18
Forsterite	127.72	289.58	55.90	352	−3.38	230	−9.58
Liebenbergite	127.72	282.75	54.83	374	−2.19	243	−8.90
Willemite	547.36	1577.8	65.31	156	−13.82	118	−15.51
Thorite	121.64	321.48	62.16	222	−10.33	156	−13.52
Titanite	155.09	370.23	58.11	306	−5.83	204	−10.97
Zircon	121.64	260.80	53.36	405	−0.56	260	−7.98
Hafnon	121.64	257.60	52.78	417	0.08	267	−7.61
Phenacite	547.36	1111.6	50.76	459	2.33	291	−6.34

ter molecules and hydroxyls are relatively small in volume, they are thus capable of diffusing easily within mineral structures with given anion porosities. By contrast, CO_2 and O_2 molecules are larger and thus difficult to migrate within the mineral structures. As a result, the rates of oxygen diffusion in minerals under anhydrous conditions are systematically lower than those under hydrothermal conditions.

If the common compensation effect holds true for both anhydrous and hydrothermal conditions, Eq. (2) can be combined with Eqs. (3) and (4) to yield the relations between anion porosities and pre-exponential factors in the form of natural logarithm:

$$\ln D_0^{dry} = -1.11\ (\pm 0.23)\Phi + 58.67\ (\pm 5.18), \quad (5)$$

and

$$\ln D_0^{wet} = -0.63\ (\pm 0.14)\Phi + 25.64\ (\pm 4.71). \quad (6)$$

Figure 3 depicts the relations between anion porosities and pre-exponential factors for the anhydrous and hydrothermal conditions, respectively. From Figs. 2 and 3 it can be seen that at $\Phi \approx 69$

Table 5. Anion porosity and oxygen diffusivity predicted for hydroxyl-bearing silicates

Mineral	V_A (Å)	V_C (Å)	Φ (%)	Q^{dry}	$\ln D_0^{dry}$	Q^{wet}	$\ln D_0^{wet}$
Pargasite	368.00	912.96	59.69	273	−7.59	185	−11.96
Tremolite	368.00	909.60	59.54	276	−7.42	187	−11.87
Cummingtonite	368.00	902.14	59.21	283	−7.05	191	−11.66
Hornblende	371.80	910.11	59.15	284	−6.99	192	−11.62
Richterite	372.56	900.54	58.62	295	−6.40	198	−11.29
Anthophyllite	736.00	1765.8	58.32	302	−6.07	201	−11.10
Glaucophene	368.00	870.83	57.74	314	−5.42	202	−10.74
Gedrite	743.60	1725.7	56.91	331	−4.50	218	−10.21
Annite	181.80	506.82	64.13	181	−12.51	132	−14.76
Phlogopite	181.80	486.60	62.64	212	−10.86	150	−13.82
Biotite	181.80	481.19	62.22	220	−10.39	155	−13.56
Muscovite	354.68	933.56	62.01	225	−10.16	158	−13.43
Lepidolite	363.60	940.38	61.33	239	−9.41	166	−13.00
Paragonite	354.68	877.51	59.58	275	−7.46	186	−11.90
Margarite	354.68	858.59	58.69	294	−6.48	197	−11.33
Lizardite	67.16	178.09	62.29	219	−10.47	154	−13.60
Serpentine	134.31	355.83	62.26	220	−10.44	155	−13.58
Chlorite	268.62	691.92	61.18	242	−9.24	167	−12.90
Amesite	268.62	688.61	60.99	246	−9.03	170	−12.78
Kaolinite	129.94	329.52	60.57	255	−8.56	175	−12.52
Talc	181.80	453.77	59.94	268	−7.86	182	−12.12
Pyrophyllite	181.80	425.16	57.24	324	−4.87	214	−10.42
Prehnite	181.51	466.01	61.05	245	−9.10	169	−12.82
Vesuvianite	1171.0	2841.8	58.79	292	−6.59	196	−11.40
Axinite	244.16	566.66	56.91	331	−4.50	218	−10.21
Humite	438.23	1014.1	56.79	333	−4.37	220	−10.14
Epidote	202.24	458.73	55.91	352	−3.39	230	−9.58
Zoisite	404.48	904.47	55.28	365	−2.69	238	−9.19
Tourmaline	702.77	1543.1	54.46	382	−1.78	247	−8.67
Chloritoid	424.83	930.08	54.32	385	−1.63	249	−8.58
Staurolite	368.74	739.94	50.17	471	2.98	298	−5.97
Topaz	174.29	346.27	49.67	481	3.54	304	−5.65

the activation energies and pre-exponential factors for hydrothermal diffusion are equal to those for anhydrous diffusion. This may imply that the rates of oxygen diffusion in minerals become identical at $\Phi \geq 69$ regardless of diffusion medium.

The linear relations in Eqs. (3) to (6) can be combined to give equations in the form of 10-based logarithm that relate oxygen diffusivity to temperature and anion porosity for the anhydrous and hydrothermal conditions, respectively:

$$\log D^{dry} = (24.70 - 0.48\Phi) - (657.3 - 9.02\Phi)10^3/RT, \quad (7)$$

and

$$\log D^{wet} = (11.14 - 0.28\Phi) - (388.7 - 5.16\Phi)10^3/RT. \quad (8)$$

The relations are valid in the temperature range of geological interest. Because the activation energy Q is in KJ/mol and D_0 is in cm^2/sec, the gas constant R is 8.3144 J/K·mol and the diffusion coefficient D is in cm^2/sec. T is the temperature in Kelvin.

Using the ionic radii of anions in Table 1, anion porosities are calculated for the minerals which include metal oxides and hydroxides, anhydrous and hydroxyl-bearing silicates, carbonates, sulfates, phosphates and wolframates. The coordination number of anions is assessed from the balance between cation and anion in given crystal structures. The coordination number of cations is available from Berry *et al.* (1983) and Smyth and Bish (1988). The coordination number of anions in question has been obtained by Zheng (1991, 1993a, 1993b) when calculating oxygen isotope fractionation in solid minerals. The calculated anion porosities together with the empirically estimated Arrhenius parameters based on Eqs. (3)

Table 6. Anion Porosity and oxygen diffusivity predicted for carbonates, sulfates, phosphates and wolframates

Mineral	V_A (Å)	V_C (Å)	Φ (%)	Q^{dry}	$\ln D_0^{dry}$	Q^{wet}	$\ln D_0^{wet}$
Calcite	136.84	367.85	62.80	208	−11.04	148	−13.92
Ankerite	143.68	326.63	56.01	350	−3.50	229	−9.65
Rhodochrosite	136.84	307.86	55.55	359	−2.99	234	−9.37
Dolomite	143.68	320.24	55.13	368	−2.52	239	−9.09
Siderite	136.84	293.17	53.32	405	−0.52	261	−7.95
Magnesite	136.84	279.05	50.25	469	2.89	297	−6.02
Witherite	95.79	303.81	68.47	91	−17.33	81	−17.50
Cerussite	95.79	269.83	64.50	173	−12.93	128	−15.00
Strontianite	95.79	255.13	62.46	215	−10.66	152	−13.71
Aragonite	95.79	226.91	57.79	313	−5.48	208	−10.78
Barite	127.72	346.97	63.19	200	−11.47	144	−14.17
Anhydrite	121.64	306.18	60.27	261	−8.23	178	−12.33
Anglesite	127.72	318.62	59.91	268	−7.83	183	−12.10
Celestite	127.72	307.96	58.53	297	−6.30	199	−11.23
Hydroxyapatite	206.41	529.09	60.99	246	−9.03	170	−12.78
Fluorapatite	204.65	523.09	60.88	248	−8.91	171	−12.71
Chlorapatite	217.10	543.01	60.02	266	−7.95	181	−12.17
Monazite	121.64	298.70	59.28	282	−7.13	190	−11.71
Xenotime	121.64	286.26	57.51	318	−5.17	211	−10.59
Scheelite	121.64	312.72	61.10	244	−9.15	168	−12.85
Huebnerite	60.82	138.39	56.05	349	−3.55	228	−9.67
Ferberite	60.82	133.58	54.47	382	−1.79	247	−8.68

to (6), are presented in Tables 3 to 6.

Equations (3) to (6) show that the porosity theory is consistent with the standard diffusion theory (Lasaga, 1981) in the following ways: (1) model Q and D_0 correlate positively with each other (Fig. 1), in keeping with the compensation relation typically observed in minerals (e.g., Winchell, 1969; Hofmann, 1980; Hart, 1981; Lasaga, 1981; Voltaggio, 1985); (2) the standard diffusion theory holds that diffusion rates in a mineral lattice are partly governed by the lattice energy (Lasaga, 1981), which is a function of M-O bond strength. This dependence is explicit in Figs. 2 and 3, where both Q and $\ln D_0$ vary inversely with Φ; (3) the diffusion theory holds that diffusion rates are largely governed by the concentration of point defects in the lattice (e.g., site vacancies). For anion diffusants like oxygen, diffusion across a crystal can be envisioned as being rate-limited not only by the energy necessary to distort the crystal lattice, but also by bonding energy of oxygen atoms to lattice vacancies and other defect sites. Therefore, an increase in lattice vacancy concentration (as monitored by an increase in Φ) represents fewer obstacles to oxygen diffusion, such that both Q and D_0 decrease by the compensation relation.

Error Analysis

Uncertainties in the empirical Arrhenius parameters for oxygen diffusion under the anhydrous and hydrothermal conditions can arise from several sources: (1) analytical errors in the experimental determination of oxygen diffusivity, (2) the assumption of a common compensation trend, (3) the use of least-squares fitting, and (4) the calculation of anion porosity and its relationship to the experimental Arrhenius parameters.

Errors associated with experimental data for oxygen diffusion in the minerals are the most fundamental to the present model. Although it cannot be resolved in this study, it is highly desirable to have the datasets of self-consistent Arrhenius parameters for species diffusion from laboratory determinations. Direct comparison between the types of diffusion experiments is also difficult because many of the early anhydrous experiments employed powdered specimens while most of the hydrothermal experiments were performed on single crystals. Furthermore, the mechanism of oxygen diffusion in minerals can vary considerably between different phases, as well as for a given phase depending on a number of factors (e.g., defect density, dislocation density, compositional variations). Oxygen diffusion is not equal for different directions in nonisometric crystals (e.g., quartz and apatite). Pressure is known to affect the magnitude of diffusion coefficients (e.g., Yund and Anderson, 1978; Ewald, 1985). The observed functional relationship between diffusion coefficients and water fugacity indicates that the diffusion of ^{18}O-labelled water controls the oxygen isotope exchange process (Farver and Yund, 1990, 1991; Zhang *et al.*, 1991). The theoretical study of McConnell (1995) indicates that the diffusion coefficients for interstitial water molecules in α-quartz are linearly related to the fugacity of external fluid phase. Further investigations are thus required to place more accurate constraints on the common compensation trend and the correlations between activation energies and anion porosities.

With respect to the compensation effect between activation energies and pre-exponential factors, Lasaga (1981) noted that the use of the compensation law in silicates and other complex phases must be modified to account for the variations in mineral structure and the types of defects. Cole and Ohmoto (1986) observed different compensation trends for oxygen diffusion in feldspars, micas, amphiboles, and carbonates. However, the inspection of all the experimental data available from literature does not allow the establishment of separate compensation lines for different minerals groups. Therefore, the common compensation trend is assumed to hold for all of the minerals regardless of the diffusion medium (Fig. 1).

The least-squares fitting has been used to regress the observed linear correlations. Despite large scatter in actual correlations (Figs. 1 and 2), much smaller errors are associated with the slopes

relative to the intercepts of the linear equations. In this regard, the activation energies derived from anion porosities are more accurate than the pre-exponential factors. Furthermore, the experimental errors in determining Q and D_0 values can be offset by the statistical regression. As a consequence, the uncertainties in the empirical activation energies (Q) and pre-exponential factors ($\ln D_0$) of Tables 3 to 6 are not worse than those from the experimental determinations.

The anion porosity in minerals is calculated from crystal-chemical parameters. It is a regorous derivation of the structural properties of minerals and thus is a predominant variable to control oxygen diffusivity in minerals. Compression and thermal expansion of the unit cell of the minerals may affect the size of anion porosities to some extent under the mantle conditions. However, errors due to the changes in the anion radii and the volume of unit cell have minimal effect on the empirical Arrhenius parameters. The relationship between the anion porosities and activation energies represented by Eqs. (3) and (4) can be changed or improved with the accumulation of experimental oxygen diffusion data in the future. Nevertheless, the values of anion porosities provide a quantitative index for comparing the relative rates of oxygen diffusion in various minerals. Even if the present model cannot predict the oxygen diffusivities for every mineral with high accuracy, it can be useful in providing a basis for understanding diffusion behaviors of the minerals having the same structural type and for extrapolation of existing data.

Discussion

In order to test the validity of the empirical estimates, comparison can be made between the predicted diffusivities and the known experimental data. Figures 4 to 7 illustrate the comparison of the empirical estimates with the experimental data available for oxygen diffusion in quartz, anorthite, diopside and magnetite.

Oxygen diffusion rates in quartz have been investigated extensively in laboratories (e.g., Giletti and Yund, 1984; Elphick *et al.*, 1986; Farver and Yund, 1991; Sharp *et al.*, 1991). In general, oxygen diffusion rates in quartz are faster and activation energies are lower under hydrothermal conditions than anhydrous conditions. As shown in Fig. 4, the independent empirical estimates in this study are in good agreement with the experimental determinations under both anhy-

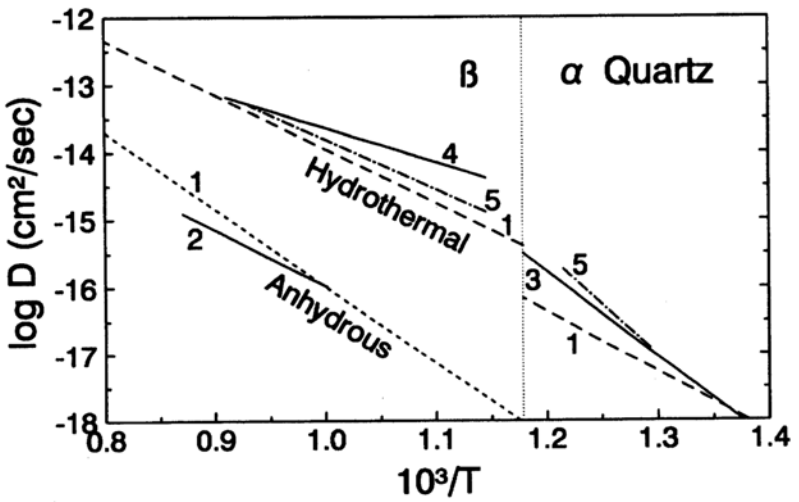

Fig. 4. Comparison of the empirical estimates with the selected experimental data for oxygen diffusion in quartz under anhydrous and hydrothermal conditions. Sources: 1 - this study, 2 - Sharp et al. (1991), 3 - Farver and Yund (1991), 4 - Elphick et al. (1986), and 5 - Giletti and Yund (1984).

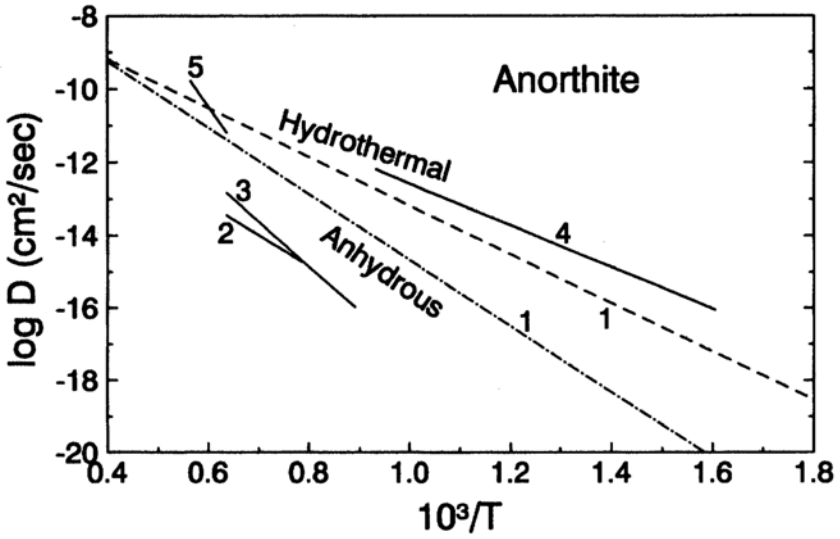

Fig. 5. Comparison of the empirical estimates with the experimental data for oxygen diffusion in anorthite under anhydrous and hydrothermal conditions. Sources: 1 - this study, 2 - Ryerson and McKeegan (1994), 3 - Elphick et al. (1988), 4 - Giletti et al. (1978), and 5 - Muehlenbachs and Kushiro (1974).

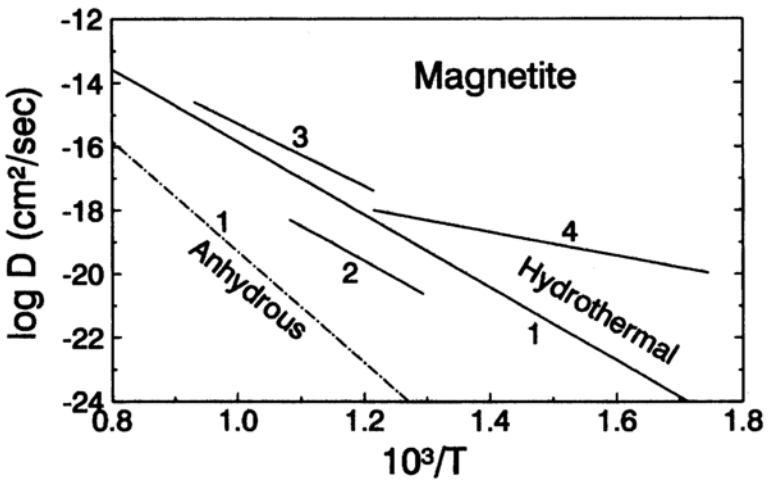

Fig. 6. Comparison of the empirical estimates with the experimental data for oxygen diffusion in magnetite under anhydrous and hydrothermal conditions. Sources: 1 - this study, 2 - Sharp (1991), 3 - Giletti and Hess (1988), and 4 - Castle and Surman (1967).

drous and hydrothermal conditions. In the experimental datasets, however, there is a difference in diffusion rates depending on orientation. The present study also indicates that differences in the distribution of anion porosities along different directions in nonisometric crystals can result in different oxygen diffusivities.

Figure 5 shows that the empirical estimates for hydrothermal oxygen diffusion in anorthite are close to the experimental data of Giletti *et al.* (1978). The good match also exists for hydrothermal oxygen diffusion in magnetite (Fig. 6). However, the rates of anhydrous oxygen diffusion in anorthite derived from this study are consider-

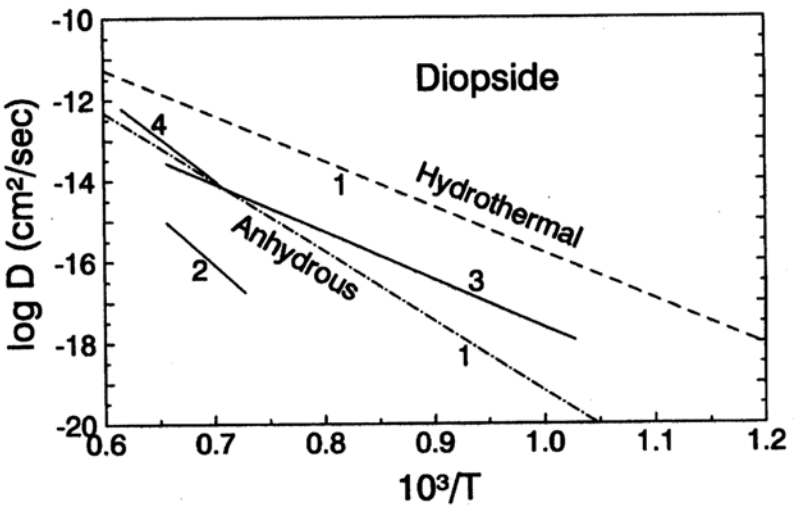

Fig. 7. Comparison of the empirical estimates with the experimental data for oxygen diffusion in diopside under anhydrous and hydrothermal conditions. Sources: 1 - this study, 2 - Ryerson and McKeegan (1994), 3 - Farver (1989), and 4 - Connolly and Muehlenbachs (1988).

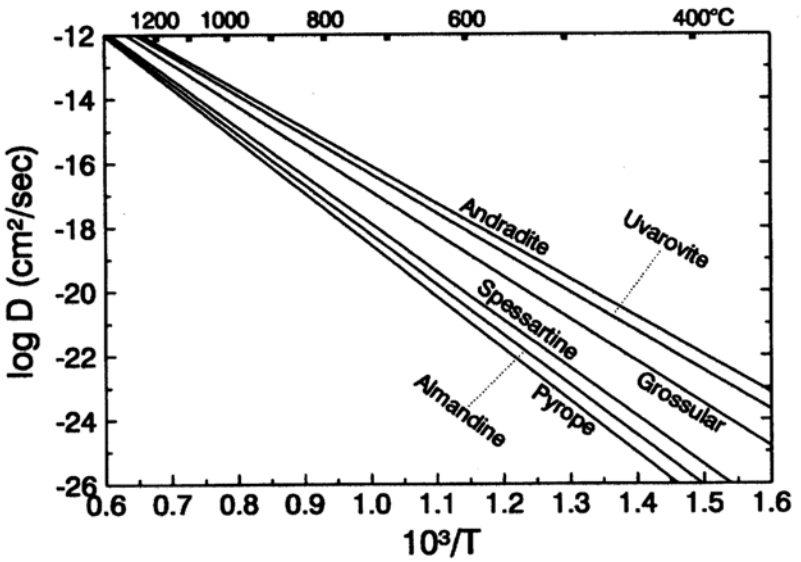

Fig. 8. Arrhenius plot of the empirically predicted oxygen diffusion in garnet minerals under hydrothermal conditions.

ably greater than the experimental determinations of Elphick *et al.* (1988) and Ryerson and McKeegan (1994). The experimental data of Farver (1989) for oxygen diffusion in diopside under hydrothermal conditions are lower than the empirical estimates in this study (Fig. 7), but they are close to the experimental data of Connolly and Muehlenbachs (1988) and the present predictions under anhydrous conditions.

Fortier and Giletti (1989) have shown that their empirical estimates for hydrothermal oxygen diffusion in common rock-forming minerals are in

fair agreement with the known experimental data. The present study further demonstrates that the anion porosity model can empirically provide an approximate estimate to oxygen diffusion coefficients for a wide range of minerals. Particularly, the anion porosities can quantify the relative sizes of the rate of oxygen diffusion in various minerals. This enables the quantitative discussion of oxygen diffusivities in the minerals.

Within each isostructural group which is characterized by the same volume of anions in the unit cell (V_A), the anion porosity varies regularly with the volume of the unit cell (V_C). Apparently, the greater the volume of the unit cell, the higher the anion porosity of a mineral and thus the greater the rates of oxygen diffusion in the mineral. Taking garnet group as example (Table 4), the volume of unit cell varies from 1753.2 Å in andradite to 1504.7 Å in pyrope, the anion porosity varies correspondingly from 56.29% to 49.07%. As shown in Fig. 8, pyrope has the lowest rates of oxygen diffusion relative to the other garnets under either anhydrous or hydrothermal conditions.

Preliminary data for oxygen diffusivity in grossular at 850 and 1050°C were reported by Freer and Dennis (1982). Their results were ambiguous because of the marked dog-leg shape of recast inverse error function profiles, possibly reflecting both volume and grain-boundary diffusions. Coghlan (1990) presented data for oxygen diffusion in spessartine-almandine at 800 to 1000°C under hydrothermal conditions. He obtained the activation energy of 301 KJ/mol and the pre-exponential factor of 6.0×10^{-5} cm^2/sec, which are comparable with the predicted Q^{wet} values of 288 to 300 KJ/mol and $D_0{}^{wet}$ values of $1.46–2.82 \times 10^{-3}$ cm^2/sec for the same compositions of garnets in this study.

For polymorphic minerals, the high pressure phase has relatively lower anion porosities and thus smaller rates for oxygen diffusion. The lowest anion porosity is 34.66% (Table 3), which is associated with stishovite, the highest pressure polymorph of SiO_2. Apparently, stishovite has the strongest Si-O bonding and thus the lowest rates of oxygen diffusion compared to the other minerals. Kyanite, the high pressure phase of Al_2SiO_5, and aragonite, the high pressure phase of $CaCO_3$, have relatively lower anion porosities (Tables 4 and 6), and therefore they diffuse oxygen in lower rates relative to the other polymorphs. In the absence of a phase change, however, the effects of compression and thermal expansion on anion porosities are relatively small.

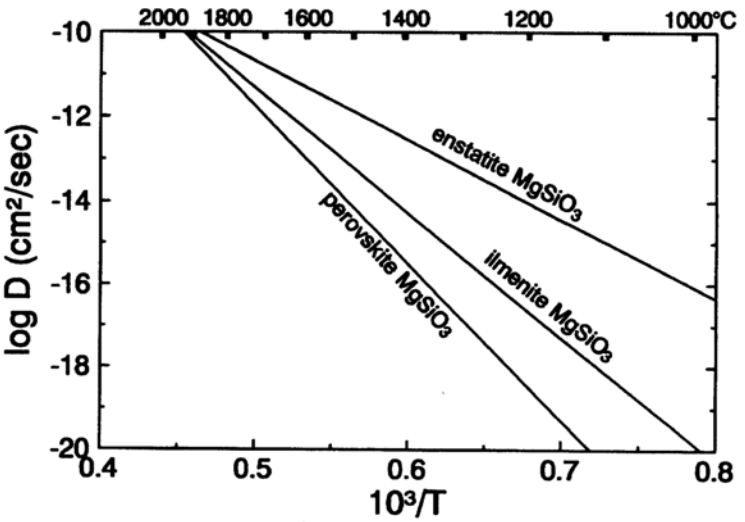

Fig. 9. Arrhenius plot of the empirically predicted oxygen diffusion in the polymorphs of $MgSiO_3$ under anhydrous conditions.

The metal oxides show a broad range of anion porosities (Table 3). In the spinels, the anion porosities range from 51.63% in spinel to 58.91% in ulvospinel. The anion porosities in the monoxides have a much broader range from 40.82% in bromellite to 69.91% in lime. It is interesting to note that the hydroxides have the anion porosities significantly higher than those of the corresponding oxides. This implies that oxygen diffusion in the hydroxides is considerably faster than that in the corresponding oxides.

Feldspathoids and pyroxenoids have higher anion porosities relative to feldspars and pyroxenes, respectively (Table 4). Correspondingly, the former groups have faster rates for oxygen diffusion relative to the later groups under the same conditions.

The ilmenite $MgSiO_3$ has an anion porosity of 45.27%, which is significantly lower than that of enstatite $MgSiO_3$ (55.44%) but higher than that of perovskite $MgSiO_3$ (38.10%). Apparently, the rates of oxygen diffusion in the ilmenite $MgSiO_3$ are smaller than those in the enstatite $MgSiO_3$ but greater than those in the perovskite $MgSiO_3$ (Fig. 9). In this regard, the rates of oxygen diffusion in the mantle could progressively decrease with increasing pressure from the upper mantle to the lower mantle. However, the rates of oxygen diffusion in minerals increase with increasing temperature. Further studies are needed to assess the effect of depth increase within the mantle (depending on changes in both pressure and temperature) on oxygen diffusivity.

The hydroxyl-bearing silicates have a relatively smaller range of anion porosities within each structural group (Table 5). Micas appear to have faster rates of oxygen diffusion relative to amphiboles under the same conditions. Topaz has the lowest anion porosity of 49.67%, and thus the rates of oxygen diffusion in it are smaller than those of the other hydroxyl-bearing silicates.

For the polymorphs of $CaCO_3$, the rates of exchange by oxygen diffusion in calcite should be faster than those in aragonite because calcite has a much higher anion porosity than aragonite (Table 6). Except calcite and aragonite, however, the other carbonates in the calcite group have lower anion porosities relative to the carbonates in the aragonite group. It is interesting that magnesite has the lowest anion porosity of 50.25% in the carbonates and thus the lowest rates of oxygen diffusion relative to the other carbonates (Fig. 10).

Oxygen isotope geothermometry has been applied to various rock type in nature. In many cases, the mineral isotope thermometry yields reasonable

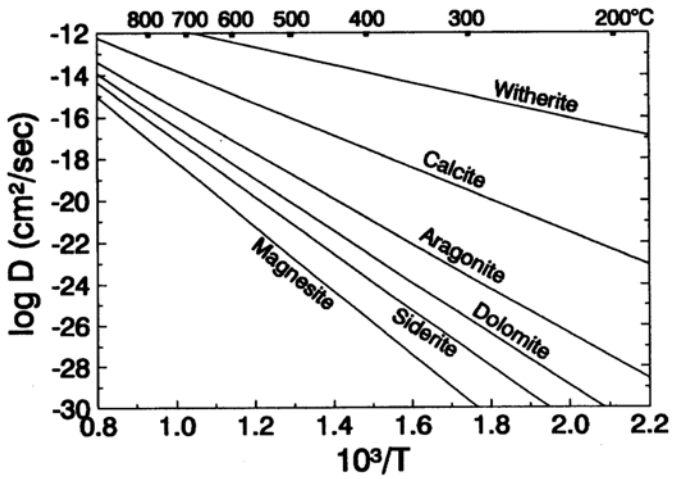

Fig. 10. Arrhenius plot of the empirically predicted oxygen diffusion in carbonate minerals under hydrothermal conditions.

temperatures in petrology (e.g., Bottinga and Javoy, 1975; Deines, 1977; Chiba *et al.*, 1989). It has been observed frequently that in slowly-cooled igneous and metamorphic rocks, isotopic temperature estimates are often lower than those from other geothermometers (e.g., Deines, 1977; Eiler *et al.*, 1993; Sharp and Jenkin, 1994). This has been ascribed to isotopic resetting associated with retrograde oxygen isotope exchange between coexisting mineral phases or with transient fluids. Giletti (1986) illustrated the cooling rate model in which oxygen diffusion data can be used in conjunction with the oxygen isotope composition of minerals to interpret apparently disequilibrium oxygen isotope fractionations in a slowly cooled mineral assemblage. The technique developed by Giletti (1986) has since been applied to place constraints on cooling rates, on the degree of deformation during retrogression, and on the presence or absence of a fluid phase during metamorphism (e.g., Jiang *et al.*, 1988; Sharp *et al.*, 1988; Jenkin *et al.*, 1991, 1994; Valley and Graham, 1991; Eiler *et al.*, 1992). With the availability of much more oxygen diffusion data derived from mineral anion porosity in this study, the application of the cooling rate model can be extended to various rocks.

Conclusions

The anion porosities of about 130 minerals have been calculated and presented along with the estimated Arrhenius parameters for oxygen self-diffusion according to a generalized empirical model. A thorough examination of the experimentally determined diffusion data demonstrates a common compensation trend between activation energies and pre-exponential factors under the anhydrous (dry) and hydrothermal (wet) conditions. However, the activation energies for hydrothermal diffusion are progressively lower than those for the anhydrous conditions with decreasing anion porosity, because water molecules and hydroxyl groups are relatively small in volume and thus easier to migrate within mineral structures with given anion porosities than carbon dioxide and oxygen molecules. This yields the two different linear trends relating activation energies and pre-exponential factors to anion porosities. At the present level of understanding and application of the diffusion data, it is probably sufficient to treat the oxygen diffusivity in minerals as if they are determined by anion porosity.

The generalized empirical model is established to describe the diffusion kinetics of oxygen in various minerals under anhydrous and hydrothermal conditions, respectively. Two sets of internally consistent data for oxygen diffusivity are yielded due to the differences in activation energies regarding the different diffusion media. It can be used to estimate diffusion coefficients for the purpose of geochemical application. It is particularly appropriate to apply the model to comparison of relative diffusivity within isostructural mineral groups. Obviously, more rigorous calculations, incorporating the other properties of material structure, and/or experimental measurements, are highly desirable. However, the results predicted in this study do appear to be reasonably concordant with available data from natural systems over a wide range of temperatures. Although the Arrhenius parameters estimated are probably not accurate enough for the precise studies of diffusion kinetics, they should be useful in guiding and extending experimental diffusion investigations and in applications to isotopic geospeedometers.

Acknowledgments—This study has been supported by the funds from the Natural Science Foundation of China and the Chinese Academy of Science within the framework of the project "Stable Isotope Geochemistry of the Earth's Crust and Mantle" (No. 49453003). Thanks are due to Drs. D. R. Baker, D. R. Cole and Z. D. Sharp as well as an anonymous reviewer for their constructive comments and to Dr. Y. Matsuhisa for his careful editing which helped improve the manuscript.

References

Anderson, T. F. (1969) Self-diffusion of carbon and oxygen in calcite by isotope exchange with carbon dioxide. *J. Geophys. Res.* **74**, 3918–3932.

Ando, K. and Oishi, Y. (1974) Self-diffusion coefficients of oxygen ion in single crystal of $MgO{\cdot}nAl_2O_3$

spinels. *J. Chem. Phys.* **61**, 625–629.

Ando, K., Kurokawa, H. and Oishi, Y. (1981) Self-diffusion coefficient of oxygen in single-crystal forsterite. *Com. Am. Ceram. Soc.* **64**, C30.

Berry, L. G., Mason, B. and Dietrich, R. V. (1983) *Mineralogy: Concepts, Descriptions and Determinations*. W. H. Freeman and Company, San Francisco, 561 pp.

Bottinga, Y. and Javoy, M. (1975) Oxygen isotope partitioning among minerals in igneous and metamorphic rocks. *Rev. Geophys. Space Phys.* **13**, 401–418.

Castle, J. E. and Surman, P. L. (1967) The self-diffusion of oxygen in magnetite: Techniques for sampling and isotopic analysis of micro quantities of water. *J. Phys. Chem.* **71**, 4255–4259.

Catlow, C. R. A. and Price, G. D. (1990) Computer modelling of solid-state inorganic materials. *Nature* **347**, 243–248.

Chiba, H., Chacko, T., Clayton, R. N. and Goldsmith, J. R. (1989) Oxygen isotope fractionations involving diopside, forsterite, magnetite, and calcite: Application to geothermometry. *Geochim. Cosmochim. Acta* **53**, 2985–2995.

Coghlan, R. A. N. (1990) Studies of diffusion transport: grain boundary transport of oxygen in feldspars, diffusion of oxygen, strontium, and REEs in garnet, and thermal histories of granitic intrusions in South-Central Maine using oxygen isotopes. Ph.D. Thesis of Brown Univ., Provindence, R.I.

Cole, D. R. and Ohmoto, H. (1986) Kinetics of isotopic exchange at elevated temperatures and pressures. *Stable Isotopes in High Temperature Geological Processes* (Valley, J. W., Taylor, H. P., Jr. and O'Neil, J. R., eds.), *Rev. Mineral.* **16**, 41–90.

Connolly, C. and Muehlenbachs, K. (1988) Contrasting oxygen diffusion in nepheline, diopside and other silicates and their relevance to isotopic systematics in meteorites. *Geochim. Cosmochim. Acta* **52**, 1585–1591.

Deines, P. (1977) On the oxygen isotope distribution among triplets in igneous and metamorphic rocks. *Geochim. Cosmochim. Acta* **41**, 1709–1730.

Dowty, E. (1980) Crystal-chemical factors affecting the mobility of ion in minerals. *Am. Mineral.* **65**, 174–182.

Eiler, J. M., Baumgartner, L. P. and Valley, J. W. (1992) Intercrystalline stable isotope diffusion: A fast boundary model. *Contrib. Mineral. Petrol.* **112**, 543–557.

Eiler, J. M., Valley, J. W. and Baumgartner, L. P. (1993) A new look at stable isotope thermometry. *Geochim. Cosmochim. Acta* **57**, 2571–2583.

Elphick, S. C., Dennis, P. F. and Graham, C. M. (1986) An experimental study of the diffusion of oxygen in quartz and albite using an overgrowth technique. *Contrib. Mineral. Petrol.* **92**, 322–330.

Elphick, S. C., Graham, C. M. and Dennis, P. F. (1988) An ion probe study of anhydrous oxygen diffusion in anorthite: A comparison with hydrothermal data and some geological implications. *Contrib. Mineral. Petrol.* **100**, 490–495.

Ewald, A. H. (1985) The effect of pressure on oxygen isotope exchange in silicates. *Chem. Geol.* **49**, 179–185.

Farver, J. R. (1989) Oxygen self-diffusion in diopside with application to cooling rate determination. *Earth Planet. Sci. Lett.* **92**, 386–396.

Farver, J. R. (1994) Oxygen self-diffusion in calcite: Dependence on temperature and water fugacity. *Earth Planet. Sci. Lett.* **121**, 575–587.

Farver, J. R. and Giletti, B. J. (1985) Oxygen diffusion in amphiboles. *Geochim. Cosmochim. Acta* **49**, 1403–1411.

Farver, J. R. and Giletti, B. J. (1989) Oxygen and strontium diffusion kinetics in apatite and their application to cooling rate determination. *Geochim. Cosmochim. Acta* **53**, 1621–1631.

Farver, J. R. and Yund, R. A. (1990) The effect of hydrogen, oxygen and water fugacity on oxygen diffusion in alkali feldspar. *Geochim. Cosmochim. Acta* **54**, 2953–2964.

Farver, J. R. and Yund, R. A. (1991) Oxygen diffusion in quartz: Dependence on temperature and water fugacity. *Chem. Geol.* **90**, 55–70.

Flygare, W. H. and Huggins, R. A. (1973) Theory of ionic transport in crystallographic tunnels. *J. Phys. Chem. Solids* **34**, 1199–1204.

Fortier, S. M. and Giletti, B. J. (1989) An empirical model for predicting diffusion coefficients in silicate minerals. *Science* **245**, 1481–1484.

Fortier, S. M. and Giletti, B. J. (1991) Volume self-diffusion of oxygen in biotite, muscovite, and phlogopite micas. *Geochim. Cosmochim. Acta* **55**, 1319–1330.

Freer, R. (1981) Diffusion in silicate minerals and glasses: A data digest and guide to the literature. *Contrib. Mineral. Petrol.* **76**, 440–454.

Freer, R. and Dennis, P. F. (1982) Oxygen diffusion studies. I. Preliminary ion microprobe investigation of oxygen diffusion in some rock-forming minerals. *Mineral. Mag.* **45**, 179–192.

Fumi, F. G. and Tosi, M. P. (1964) Ionic sizes and Born repulsive parameters in the NaCl-type alkali halides. *J. Phys. Chem. Solids* **25**, 31–52.

Gautason, B. and Muehlenbachs, K. (1993) Oxygen diffusion in perovskite: Implications for electrical conductivity in the lower mantle. *Science* **260**, 518–

521.

Giletti, B. J. (1985) The nature of oxygen transport within minerals in the presence of hydrothermal water and the role of diffusion. *Chem. Geol.* **53**, 197–206.

Giletti, B. J. (1986) Diffusion effects on oxygen isotope temperatures of slowly cooled igneous and metamorphic rocks. *Earth Planet. Sci. Lett.* **77**, 218–228.

Giletti, B. J. and Hess, K. C. (1988) Oxygen diffusion in magnetite. *Earth Planet. Sci. Lett.* **89**, 115–122.

Giletti, B. J. and Yund, R. A. (1984) Oxygen diffusion in quartz. *J. Geophys. Res.* **B89**, 4039–4046.

Giletti, B. J., Semet, M. P. and Yund, R. A. (1978) Studies in diffusion, III. Oxygen in feldspars, an ion microprobe determination. *Geochim. Cosmochim. Acta* **42**, 45–57.

Hart, S. R. (1981) Diffusion compensation in natural silicates. *Geochim. Cosmochim. Acta* **45**, 279–291.

Hayashi, T. and Muehlenbachs, K. (1986) Rapid oxygen diffusion in melilite and its relevance to meterorites. *Geochim. Cosmochim. Acta* **50**, 585–591.

Hofmann, A. W. (1980) Diffusion in natural silicate melts: A critical review. *Physics of Magmatic Processes* (Hargraves, R., ed.), 385–417, Princeton Univ. Press.

Jaoul, O., Houlier, B. and Abel, F. (1983) Study of ^{18}O diffusion in magnesium orthosilicate by nuclear microanalysis. *J. Geophys. Res.* **B88**, 613–624.

Jenkin, G. R. T., Linklater, C. and Fallick, A. E. (1991) Modelling of mineral ^{18}O values in an igneous aureole: closed-system model predicts apparent open-system $\delta^{18}O$ values. *Geology* **19**, 1185–1188.

Jenkin, G. R. T., Farrow, C. M., Fallick, A. E. and Higgins, D. (1994) Oxygen isotope exchange and closure temperatures in cooling rocks. *J. Metamorph. Geol.* **12**, 221–235.

Jiang, J.-X., Clayton, R. N. and Newton, R. C. (1988) Fluids in granulite facies metamorphism: A comparative oxygen isotope study of the South India and Adirondack high-grade terrains. *J. Geol.* **96**, 517–533.

Kronenberg, A. K., Yund, R. A. and Giletti, B. J. (1984) Carbon and oxygen diffusion in calcite: Effects of Mn and P_{H_2O}. *Phys. Chem. Mineral.* **11**, 101–112.

Lasaga, A. C. (1981) The atomistic basis of kinetics: defects in minerals. *Kinetics of Geochemical Processes* (Lasaga, A. C. and Kirkpatrick, R. J., eds.), *Rew. Mineral.* **8**, 261–321.

McConnell, J. D. C. (1995) The role of water in oxygen isotope exchange in quartz. *Earth Planet. Sci. Lett.* **136**, 97–107.

Muehlenbachs, K. and Connolly, C. (1991) Oxygen diffusion in leucite: Structural controls. *Stable Isotope Geochemistry: A Tribute to Samuel Epstein* (Taylor, H. P., Jr., O'Neil, J. R. and Kaplan, I. R., eds.), Geochem. Soc. Spec. Publ. No. 3, 27–34.

Muehlenbachs, K. and Kushiro, I. (1974) Oxygen isotope exchange and equilibrium of silicates with CO_2 or O_2. *Carnegie Institution Washington Yearbook* **73**, 232–240.

Muller, O. and Roy, R. (1974) *The Major Ternary Structural Families*. Springer-Verlag, Berlin Heidelberg New York, 487 pp.

Patel, A., Price, G. D. and Mendelssohn, M. J. (1991) A computer simulation approach to modelling the structure, thermodynamics and oxygen isotope equilibria of silicates. *Phys. Chem. Mineral.* **17**, 690–699.

Purton, J. and Catlow, C. R. A. (1990) Computer simulation of feldspar structures. *Am. Mineral.* **75**, 1268–1273.

Reddy, K. P. R. and Cooper, A. R. (1982) Oxygen diffusion in sapphire. *J. Am. Ceram. Soc.* **65**, 634–638.

Reddy, K. P. R. and Cooper, A. R. (1983) Oxygen diffusion in MgO and α-Fe_2O_3. *J. Am. Ceram. Soc.* **66**, 664–666.

Ryerson, F. J. and McKeegan, K. D. (1994) Determination of oxygen self-diffusion in akermanite, anorthite, diopside, and spinel: Implications for oxygen isotope anomalies and the thermal histories of Ca-Al-rich inclusions. *Geochim. Cosmochim. Acta* **58**, 3713–3734.

Shannon, R. D. (1976) Revised effective ionic radii and systematic studies of interatomic distances in halides and chalcogenides. *Acta Cryst.* **A32**, 751–767.

Shannon, R. D. and Prewitt, C. T. (1969) Effective ionic radii in oxides and fluorides. *Acta Cryst.* **B25**, 925–945.

Sharp, Z. D. (1991) Determination of oxygen diffusion rates in magnetite from natural isotopic variations. *Geology* **19**, 653–656.

Sharp, Z. D. and Jenkin, G. R. T. (1994) An empirical estimate of the diffusion rate of oxygen in diopside. *J. Metamorph. Geol.* **12**, 89–97.

Sharp, Z. D., O'Neil, J. R. and Essene, E. J. (1988) Oxygen isotope variations in granulite-grade iron formation: constraints on oxygen diffusion and retrograde isotopic exchange. *Contrib. Mineral. Petrol.* **98**, 490–501.

Sharp, Z. D., Giletti, B. J. and Yoder, H. S., Jr. (1991) Oxygen diffusion rates in quartz exchanged with CO_2. *Earth Planet. Sci. Lett.* **107**, 339–348.

Smyth, J. R. and Bish, D. L. (1988) *Crystal Structures and Cation Sites of the Rock-Forming Minerals*. Allen and Unwin, Boston, 332 pp.

Valley, J. W. and Graham, C. M. (1991) Ion microprobe analysis of oxygen isotope ratios in granulite facies magnetites: diffusive exchange as a guide to cooling

history. *Contrib. Mineral. Petrol.* **109**, 38–52.

Vocadlo, L., Wall, A., Parker, S. C. and Price, G. D. C. (1995) Absolute ionic diffusion in MgO—Computer calculations via lattice dynamics. *Phys. Earth Planet. Inter.* **88**, 193–210.

Voltaggio, M. (1985) Estimation of diffusion constants by observations of isokinetic effects: A test for radiogenic argon and strontium. *Geochim. Cosmochim. Acta* **49**, 2117–2122.

Winchell, P. (1969) The compensation law for diffusion in silicates. *High Temp. Sci.* **1**, 200–215.

Wright, K. and Catlow, C. R. A. (1994) A computer simulation of OH defects in olivine. *Phys. Chem. Mineral.* **20**, 515–518.

Wright, K., Freer, R. and Catlow, C. R. A. (1995) Oxygen diffusion in grossular and some geological implications. *Am. Mineral.* **80**, 1020–1025.

Wright, K., Freer, R. and Catlow, C. R. A. (1996) Water-related defects and oxygen diffusion in albite: a computer simulation study. *Contrib. Mineral. Petrol.* **125**, 161–166.

Yund, R. A. and Anderson, T. F. (1978) Oxygen isotope exchange between feldspar and fluid as a function of fluid pressure. *Geochim. Cosmochim. Acta* **42**, 235–239.

Zhang, Y.-X., Stolper, E. M. and Wasserburg, G. J. (1991) Diffusion of a multi-species component and its role in oxygen and water transport in silicates. *Earth Planet. Sci. Lett.* **103**, 228–240.

Zheng, Y.-F. (1991) Calculation of oxygen isotope fractionation in metal oxides. *Geochim. Cosmochim. Acta* **55**, 2299–2307.

Zheng, Y.-F. (1993a) Calculation of oxygen isotope fractionation in anhydrous silicate minerals. *Geochim. Cosmochim. Acta* **57**, 1079–1091.

Zheng, Y.-F. (1993b) Calculation of oxygen isotope fractionation in hydroxyl-bearing silicates. *Earth Planet. Sci. Lett.* **120**, 247–263.